

Magnetism: Molecules to Materials IV

Nanosized Magnetic Materials

Edited by
Joel S. Miller and Marc Drillon

 **WILEY-VCH**

Magnetism: Molecules to Materials IV

Edited by J. S. Miller and M. Drillon

 **WILEY-VCH**

Further Titles of Interest

J. S. Miller and M. Drillon (Eds.)
Magnetism: Molecules to Materials
Models and Experiments
2001. XVI, 437 pages
Hardcover. ISBN: 3-527-29772-3

J. S. Miller and M. Drillon (Eds.)
Magnetism: Molecules to Materials II
Molecule-Based Materials
2001. XIV, 489 pages
Hardcover. ISBN: 3-527-30301-4

J. H. Fendler (Ed.)
Nanoparticles and Nanostructured Films
1998. XX, 468 pages
Hardcover. ISBN: 3-527-29443-0

P. Braunstein, L. A. Oro, and P. R. Raithby (Eds.)
Metal Clusters in Chemistry
1999. XLVIII, 1798 pages
ISBN: 3-527-29549-6

Magnetism: Molecules to Materials IV

Nanosized Magnetic Materials

Edited by
Joel S. Miller and Marc Drillon

 **WILEY-VCH**

Prof. Dr. Joel S. Miller
University of Utah
315 S. 1400 E. RM Dock
Salt Lake City
UT 84112-0850
USA

Prof. Dr. Marc Drillon
CNRS
Inst. de Physique et Chimie
des Matériaux de Strasbourg
23 Rue du Loess
67037 Strasbourg Cedex
France

This book was carefully produced. Nevertheless, editors, authors and publisher do not warrant the information contained therein to be free of errors. Readers are advised to keep in mind that statements, data, illustrations, procedural details or other items may inadvertently be inaccurate.

Library of Congress Card No.: applied for

A catalogue record for this book is available from the British Library.

Die Deutsche Bibliothek - CIP Cataloguing-in-Publication-Data

A catalogue record for this publication is available from Die Deutsche Bibliothek

ISBN 3-527-30429-0

© WILEY-VCH Verlag GmbH, Weinheim (Federal Republic of Germany). 2002

Printed on acid-free paper.

All rights reserved (including those of translation in other languages). No part of this book may be reproduced in any form - by photoprinting, microfilm, or any other means - nor transmitted or translated into machine language without written permission from the publishers. Registered names, trademarks, etc. used in this book, even when not specifically marked as such, are not to be considered unprotected by law.

Composition: EDV-Beratung Frank Herweg, Leutershausen. Printing: betz-druck GmbH, Darmstadt. Bookbinding: Wilh. Osswald + Co. KG, Neustadt
Printed in the Federal Republic of Germany.

Preface

The development, characterization, and technological exploitation of new materials, particularly as components in 'smart' systems, are key challenges for chemistry and physics in the next millennium. New substances and composites including nanostructured materials are envisioned for innumerable areas including magnets for the communication and information sector of our economy. Magnets are already an important component of the economy with worldwide sales of approximately \$30 billion, twice that of the sales of semiconductors. Hence, research groups worldwide are targeting the preparation and study of new magnets especially in combination with other technologically important properties, e. g., electrical and optical properties.

In the past few years our understanding of magnetic materials, thought to be mature, has enjoyed a renaissance as it is being expanded by contributions from many diverse areas of science and engineering. These include (i) the discovery of bulk ferro- and ferrimagnets based on organic/molecular components with critical temperature exceeding room temperature, (ii) the discovery that clusters in high, but not necessarily the highest, spin states due to a large magnetic anisotropy or zero field splitting have a significant relaxation barrier that traps magnetic flux enabling a single molecule/ion (cluster) to act as a magnet at low temperature; (iii) the discovery of materials exhibiting large, negative magnetization; (iv) spin-crossover materials that can show large hysteretic effects above room temperature; (v) photomagnetic and (vi) electrochemical modulation of the magnetic behavior; (vii) the Haldane conjecture and its experimental realization; (viii) quantum tunneling of magnetization in high spin organic molecules; (viii) giant and (ix) colossal magnetoresistance effects observed for 3-D network solids; (x) the realization of nanosize materials, such as self organized metal-based clusters, dots and wires; (xi) the development of metallic multilayers and the spin electronics for the applications. This important contribution to magnetism and more importantly to science in general will lead us into the next millennium.

Documentation of the status of research, ever since William Gilbert's *de Magnete* in 1600, provides the foundation for future discoveries to thrive. As one millennium ends and another beacons the time is appropriate to pool our growing knowledge and assess many aspects of magnetism. This series entitled *Magnetism: Molecules to Materials* provides a forum for comprehensive yet critical reviews on many aspects of magnetism that are on the forefront of science today.

Joel S. Miller
Salt Lake City, USA

Marc Drillon
Strasbourg, France

Contents

Preface	V
List of Contributors	XV
1 Bimetallic Magnets: Present and Perspectives	1
1.1 Introduction	1
1.2 Bimetallic Magnetic Materials Derived from Oxamato-based Complexes	2
1.2.1 Dimensionality and Magnetic Properties	2
1.2.2 Modulation of the Magnetic Properties	17
1.2.3 Dimensionality Modulation by a Dehydration-Polymerization Process	20
1.2.4 Alternative Techniques for the Studies of Exchange-coupled Systems	26
1.3 Bimetallic Magnets Based on Second- and Third-row Transition Metal Ions	28
1.3.1 Examples of Ru(III)-based Compounds	28
1.3.2 Mo, Nb, and W-cyanometalate-based Magnets	31
1.3.3 Light-induced Magnetism	36
1.4 Concluding Remarks	37
References	38
2 Copper(II) Nitroxide Molecular Spin-transition Complexes	41
2.1 Introduction	41
2.2 Nitroxide Free Radicals as Building Blocks for Metal-containing Magnetic Species	42
2.2.1 Electronic Structure	43
2.2.2 Coordination Properties	43
2.3 Molecular Spin Transition Species	46
2.3.1 Discrete Species	46
2.3.2 One-dimensional Species	50
2.4 Conclusion	61
References	62
3 Theoretical Study of the Electronic Structure of and Magnetic Interactions in Purely Organic Nitronyl Nitroxide Crystals	65
3.1 Introduction	65
3.2 Electronic Structure of Nitronyl Nitroxide Radicals	68

3.2.1	Fundamentals	68
3.2.2	<i>Ab-initio</i> Computation of the Electronic Structure of Nitronyl Nitroxide Radicals	73
3.2.3	Spin Distribution in Nitronyl Nitroxide Radicals	78
3.3	Magnetic Interactions in Purely Organic Molecular Crystals	88
3.3.1	Basics of the Magnetism in Purely Organic Molecular Crystals	88
3.3.2	The McConnell-I Mechanism: A Rigorous Theoretical Analysis	90
3.3.3	Theoretical Analysis of Through-space Intermolecular Interactions	94
3.3.4	Experimental Magneto-structural Correlations	102
3.3.5	Theoretical Magneto-structural Correlations	105
	References	113
4	Exact and Approximate Theoretical Techniques for Quantum Magnetism in Low Dimensions	119
4.1	Introduction	119
4.2	Exact Calculations	121
4.3	Applications to Spin Clusters	125
4.4	Field Theoretic Studies of Spin Chains	129
4.4.1	Nonlinear σ -model	130
4.4.2	Bosonization	133
4.5	Density Matrix Renormalization Group Method	137
4.5.1	Implementation of the DMRG Method	139
4.5.2	Finite Size DMRG Algorithm	140
4.5.3	Calculation of Properties in the DMRG Basis	142
4.5.4	Remarks on the Applications of DMRG	142
4.6	Frustrated and Dimerized Spin Chains	144
4.7	Alternating (S_1, S_2) Ferrimagnetic Spin Chains	148
4.7.1	Ground State and Excitation Spectrum	149
4.7.2	Low-temperature Thermodynamic Properties	155
4.8	Magnetization Properties of a Spin Ladder	160
	References	168
5	Magnetic Properties of Self-assembled [2×2] and [3×3] Grids	173
5.1	Introduction	173
5.2	Polytopic Ligands and Grid Complexes	174
5.2.1	[2×2] Ligands	175
5.2.2	Representative [2×2] Complexes	176
5.2.3	[3×3] Ligands and their Complexes	187
5.3	Magnetic Properties of Grid Complexes	189
5.3.1	[2×2] Complexes	189
5.3.2	[3×3] Complexes	191
5.3.3	Magnetic Properties of [2×2] and [3×3] Grids	192

5.3.4	Potential Applications of Magnetic Grids to Nanoscale Technology	201
References	202
6	Biogenic Magnets	205
6.1	Introduction	205
6.1.1	Magnetotactic Bacteria	205
6.1.2	Magnetosomes	206
6.1.3	Magnetite Magnetosomes	207
6.1.4	Greigite Magnetosomes	208
6.2	Magnetic Properties of Magnetosomes	209
6.2.1	Magnetic Microstates and Crystal Size	209
6.2.2	Single-domain (SD) and Multi-domain (MD) States	211
6.2.3	Superparamagnetic (SPM) State	211
6.2.4	Theoretical Domain Calculations: Butler–Banerjee Model	213
6.2.5	Local Energy Minima and Metastable SD States: Micromagnetic Models	214
6.2.6	Magnetic Anisotropy of Magnetosomes	215
6.2.7	Magnetosome Chains	217
6.2.8	Magnetic Properties of Magnetosomes at Ambient Temperatures	217
6.2.9	Low-temperature (<300 K) Magnetic Properties	218
6.2.10	Magnetosomes and Micromagnetism	220
6.2.11	Magnetosome Magnetization from Electron Holography	220
6.3	Mechanism of Bacterial Magnetotaxis	223
6.3.1	Passive Orientation by the Geomagnetic Field	223
6.3.2	Magneto-aerotaxis	225
6.4	Conclusion	227
References	228
7	Magnetic Ordering due to Dipolar Interaction in Low Dimensional Materials	233
7.1	Introduction	233
7.2	Magnetic Ordering in Pure Dipole Systems	234
7.2.1	The Dipole–Dipole Interaction – A Well Known Hamiltonian?	234
7.2.2	Ordering Temperature – The Mean-field Approach	235
7.2.3	Dipolar Ordering in 3D Systems	238
7.2.4	Dipolar Ordering in 2D Systems	243
7.3	Strongly Correlated Extended Objects	246
7.3.1	Stacking of Magnetic Planes	246
7.3.2	3D of 1D – Bunching of Wires or Chains	248
7.3.3	2D of 1D – Planar Arrays of Magnetic Wires	250
7.3.4	2D of 0D – Planar Arrays of Magnetic Dots	252
7.3.5	1D of 0D – Lines of Magnetic Dots	254
7.4	Weakly Correlated Extended Systems	255

7.4.1	Low Dimensional Molecular-based Magnets	255
7.4.2	3D Ordering Due to Dipolar Interaction – A Model	261
7.5	Conclusion	265
	References	266
8	Spin Transition Phenomena	271
8.1	Introduction	271
8.2	Physical Characterization	272
8.2.1	Occurrence of Thermal Spin Transition	272
8.2.2	Magnetic Susceptibility Measurements	274
8.2.3	Optical Spectroscopy	275
8.2.4	Vibrational Spectroscopy	276
8.2.5	⁵⁷ Fe Mössbauer Spectroscopy	277
8.2.6	Calorimetry	279
8.2.7	Diffraction Methods	280
8.2.8	X-ray Absorption Spectroscopy	281
8.2.9	Positron-annihilation Spectroscopy	282
8.2.10	Nuclear Resonant Scattering of Synchrotron Radiation	283
8.2.11	Magnetic Resonance Studies (NMR, EPR)	284
8.3	Highlights of Past Research	285
8.3.1	Chemical Influence on Spin-crossover Behavior	285
8.3.2	Structural Insights	289
8.3.3	Influence of Crystal Quality	291
8.3.4	Theoretical Approaches to Spin Transition Phenomena	292
8.3.5	Influence of a Magnetic Field	299
8.3.6	Two-step Spin Transition	299
8.3.7	LIESST Experiments	306
8.3.8	Formation of Correlations During HS → LS relaxation	309
8.3.9	Nuclear Decay-induced Spin Crossover	313
8.4	New Trends in Spin Crossover Research	320
8.4.1	New Types of Spin Crossover Material	320
8.4.2	New Effects and Phenomena	326
	References	334
9	Interpretation and Calculation of Spin-Hamiltonian Parameters in Transition Metal Complexes	345
9.1	Introduction	345
9.2	The Spin-Hamiltonian	347
9.2.1	The SH	347
9.2.2	Eigenstates of the SH	348
9.2.3	Matrix Elements of the SH	349
9.2.4	Comments	352
9.3	The Physical Origin of Spin-Hamiltonian Parameters	352
9.3.1	Many-electron Wavefunctions and the Zeroth-order Hamiltonian	352
9.3.2	Perturbing Operators for Magnetic Interactions	355
9.3.3	Theory of Effective Hamiltonians	361

9.3.4	Equations for Spin-Hamiltonian Parameters	363
9.3.5	Formulation in Terms of Molecular Orbitals	371
9.4	Ligand Field and Covalency Effects on SH Parameters	380
9.4.1	Molecular Orbitals for Inorganic Complexes	380
9.4.2	Ligand Field Energies	381
9.4.3	Matrix Elements over Molecular Orbitals	385
9.4.4	“Central Field” versus “Symmetry Restricted” Covalency	392
9.4.5	Ligand-field Theory of Zero-field Splittings	395
9.4.6	Ligand-field Theory of the g-Tensor	396
9.4.7	Ligand-field Theory of Hyperfine Couplings	397
9.4.8	Table of Hyperfine Parameters	399
9.4.9	Examples of Ligand-field Expressions for Spin Hamiltonian Parameters	401
9.5	Case Studies of SH Parameters	414
9.5.1	CuCl_4^{2-} and the Blue Active Site: g and A^M Values	415
9.5.2	FeCl_4^- and the $\text{Fe}(\text{SR})_4^-$ Active Site: Zero-field Splitting (ZFS)	420
9.6	Computational Approaches to SH Parameters	423
9.6.1	Hartree–Fock Theory	424
9.6.2	Configuration Interaction	426
9.6.3	Density Functional Theory	427
9.6.4	Coupled-perturbed SCF Theory	428
9.6.5	Relativistic Methods	432
9.6.6	Calculation of Zero-field Splittings	433
9.6.7	Calculation of g-Values	435
9.6.8	Calculation of Hyperfine Couplings	444
9.7	Concluding Remarks	455
9.8	Appendix: Calculation of Spin–Orbit Coupling Matrix Elements	456
	References	458
10	Chemical Reactions in Applied Magnetic Fields	467
10.1	Introduction	467
10.2	Gas-phase Reactions	467
10.2.1	Gaseous Combustion	467
10.2.2	Carbon Nanotube and Fullerene Synthesis	468
10.2.3	Liquid-phase Reactions	470
10.2.4	Asymmetric Synthesis	470
10.2.5	Electrodeposition	471
10.3	Solid-phase Reactions	472
10.3.1	Self-propagating High-temperature Synthesis (SHS)	472
10.3.2	SHS Reactions in High Fields (1 to 20 T)	475
10.3.3	Time-resolved X-ray Diffraction Studies	476
10.3.4	Possible Field-dependent Reaction Mechanisms	479
10.4	Conclusions	479
	References	480
	Index	483

List of Contributors

Prof. Richard B. Frankel
Physics Department
California Polytechnic State University
San Luis Obispo, CA 93407
USA

Prof. Bruce M. Moskowitz
Department of Geology and Geophysics
University of Minnesota
310 Pillsbury Drive SE
Minneapolis, MN 55455
USA

Yann Garcia, Hartmut Spiering,
Prof. Philipp Gütllich
Institute of Inorganic Chemistry
and Analytical Chemistry
Johannes Gutenberg University
Staudingerweg 9
55099 Mainz
Germany

Prof. Juan J. Novoa, Pilar Lafuente,
Prof. Mercè Deumal
Departament de Química Física,
Facultat de Química, and
CER de Química Teòrica,
Universitat de Barcelona,
Av. Diagonal 647
08028-Barcelona
Spain

Prof. Fernando Mota
Department of Chemistry
King's College London, Strand
London WC2R 2LS
UK

Prof. Pierre Panissod,
Prof. Marc Drillon
Institut de Physique et Chimie des
Matériaux de Strasbourg,
UMR CNRS 75040
23 rue du Loess
67037 Strasbourg
France

Dr. Quentin A. Pankhurst
Department of Physics and Astronomy
University College London
Gower Street
London WC1E 6BT
UK

Prof. Ivan P. Parkin
Department of Chemistry
University College London
20 Gordon Street
London WC1H 0AJ
UK

Dr. Paul Rey
CEA-Département de Recherche
Fondamentale sur la Matière Condensée
Service de Chimie Inorganique
et Biologique
Laboratoire de Chimie de Coordination
UMR CNRS 5046
17 rue des Martyrs
38054 Grenoble cedex 09
France

XIV List of Contributors

Prof. Victor I. Ovcharenko
Laboratory of polypyrrole compounds
International Tomography Center
Institutskaya 3A
630090 Novosibirsk
Russia

Dr. Frank Neese
Max-Planck-Institut für Strahlenchemie
Stiftstr. 34–36
45470 Mülheim/Ruhr
Germany

Prof. Edward I. Solomon
Stanford University
Department of Chemistry
Stanford, CA, 94305
USA

Prof. Olivier Kahn (deceased)
Prof. Corine Mathonière,
Dr. Jean-Pascal Sutter
Groupe des Sciences Moléculaires
Institut de Chimie de la Matière
Condensée de Bordeaux
CNRS
F-33608 Pessac
France

Dr. Jatinder V. Yakhmi
Technical Physics & Prototype
Engineering Division
Physics Group
Bhabha Atomic Research Center
Mumbai (Bombay) – 400 085
India

Prof. S. Ramasesha
Solid State & Structural Chemistry Unit
Indian Institute of Science
Bangalore 560 012
India

Prof. Laurence K. Thompson,
Zhiqiang Xu
Department of Chemistry
Memorial University of Newfoundland
St. John's, Newfoundland, A1B 3X7
Canada

Dr. Oliver Waldmann
Physikalisches Institut III
Universität Erlangen-Nürnberg
Erwin-Rommel-Str. 1
91058 Erlangen
Germany

1 Bimetallic Magnets: Present and Perspectives

Corine Mathonière, Jean-Pascal Sutter, and Jatinder V. Yakhmi

1.1 Introduction

An important branch of the molecular magnetism deals with molecular systems with bulk physical properties such as long-range magnetic ordering. The first molecular compounds with spontaneous magnetization below a critical temperature were reported during the eighties [1, 2]. These pioneering reports encouraged many research groups in organic, inorganic, or organometallic chemistry to initiate activity on this subject, and many new molecule-based magnets have been designed and characterized. A tentative classification can arise from the chemical nature of the magnetic units involved in these materials – organic- or metal-based systems and mixed organic–inorganic compounds. Of materials based only on magnetic metal complexes, several families such as the oxamato, oxamido, oxalato-bridged compounds and cyanide-bridged systems play an important role in the field of molecular magnetism. This contribution focuses mainly on molecule-based magnets involving oxamato and oxamido complexes. The most extensively used spin carriers are 3d transition metal ions. The magnetic interactions between these ions are now well understood and enable the rational synthesis of materials. This aspect will be highlighted in the first part of this contribution. The heavier homologs from the second and third series have been envisaged only recently for the construction of heterobimetallic materials. In the second part of this chapter we will briefly discuss the very encouraging first results obtained with such ions.

In 1995 Olivier Kahn wrote a paper reviewing the magnetism of heterobimetallic compounds [3]. An important part of this review was devoted to finite polynuclear compounds, which can be considered as models for the study of exchange interactions. Magnetic ordering is a three dimensional property, however, and the design of a molecule-based magnet requires control of the molecular architecture in the three directions of space. The results obtained in bimetallic supra-molecular materials by our group and others show different features:

- the dimensionality can be controlled by the stoichiometry of the reagents during the synthesis or by the number of solvation molecules;

¹ This chapter is dedicated to the memory of Professor Olivier Kahn who passed away suddenly on December 8, 1999. Many of the illustrative examples used in this contribution are results obtained by his group.

- in a chemical system, the magnetic properties can be modulated by the nature of metallic ions;
- these systems can be studied by alternative techniques which are complementary of the magnetic studies.

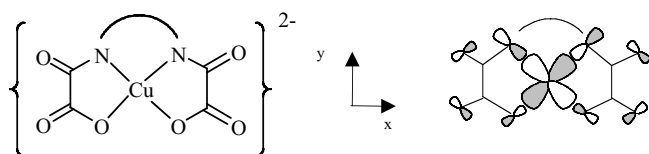
In the following text we will describe briefly the structures and magnetic properties of the compounds by emphasizing their main features. In particular, the magnetic properties will be summarized in terms of the exchange parameter J , the ordering temperature, T_C for a ferro(or ferri)magnetic material or T_N for an antiferromagnetic material, and the coercive field H_{coerc} , i. e. the magnetic field applied to cancel the permanent magnetization present in the material, which characterizes the hardness of a magnet.

1.2 Bimetallic Magnetic Materials Derived from Oxamato-based Complexes

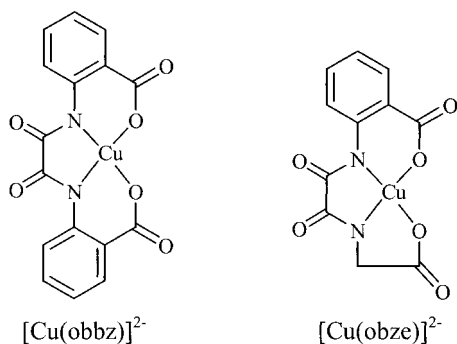
1.2.1 Dimensionality and Magnetic Properties

1.2.1.1 Cu^{II} Precursors

The general chemical strategy for the construction of bimetallic systems is based on the use of the bis-bidentate metal-complex as a complex-ligand. The bis-oxamato Cu precursors (shown in Scheme 1) and disymmetrical Cu^{II} complexes with two types of bridging units (oxamato and carboxylato) (shown in Scheme 2) have mainly been used for the preparation of extended bimetallic compounds.



Scheme 1



Scheme 2

$[\text{Cu}(\text{pba})]^{2-}$ (Table 1) was first described by Nonoyama in 1976 [4] and at the end of the eighties it was used by Kahn and coworkers to design high-spin molecules, namely $(\text{LM})_2\text{Cu}(\text{pba})$ with $\text{M} = \text{Mn}^{\text{II}}, \text{Ni}^{\text{II}}$, L being a terminal ligand or bimetallic chains $\text{MCu}(\text{pba})$ [5, 6]. $[\text{Cu}(\text{opba})]^{2-}$ was later synthesized by Stumpf; this precursor enables the preparation of compounds with different dimensionality – high-spin molecules [7], chain and ladders compounds, honeycomb layers, and interlocked compounds (Table 1) [8].

These Cu precursors were chemically modified through their ligand skeleton. The pba and opba ligands have been modified in two directions (Table 1):

- in the bridging moiety, by substituting the O (R_1 and R_2) atoms by N atoms, to increase the overlap of magnetic orbitals, because of the more pronounced diffuse character of the $2p(\text{N})$ orbitals (next section);
- around the bridging moiety, by changing the nature of the R unit to modify the crystal packing of the molecules.

1.2.1.2 Mechanisms of Exchange Coupling

In the bimetallic systems obtained from reaction of Cu^{II} compounds with other transition metal ions, M, the magnetic ordering is ferrimagnetic. This means that exchange interactions between Cu and M ($S_{\text{Cu}} \neq S_{\text{M}}$ with S referring to the spin state of the metal) in the systems are a result of overlap between magnetic orbitals. If M has no orbital contribution (magnetically isotropic ion), the mechanism of the dominant $\text{Cu}^{\text{II}}\text{--M}$ interactions through an oxamato (or oxamido)-bridge is well understood. In fact, both the planar structure of the Cu^{II} complex and the four peripheral oxygen atoms give to the compound its efficient mediating character in terms of magnetic connector. The Cu^{II} ion has one unpaired electron occupying a d_{xy} orbital which is delocalized toward the nearest nitrogen and oxygen atoms and also toward the external oxygen atoms (Scheme 1). This magnetic orbital may overlap strongly with magnetic orbitals of other ions linked to the Cu^{II} brick by the four external oxygen atoms. Structural investigations of several compounds in this family have shown that the distances between the two metals, $\text{Cu}^{\text{II}}\text{--M}$, is approximately 5.3 Å. Going further in the quantification of the exchange interactions, the magnetic data can be interpreted in the paramagnetic regime with a phenomenological Hamiltonian in a spin-spin coupling scheme such as $H = -J\mathbf{S}_{\text{Cu}} \cdot \mathbf{S}_{\text{M}}$, where J is the isotropic interaction parameter. For example, in $\text{Cu}^{\text{II}}\text{--Mn}^{\text{II}}$ pairs, J has been found to be approximately -30 cm^{-1} . On the basis of experimental studies (magnetism and neutron diffraction) and theoretical investigations (DFT calculations), the dominant mechanism is spin delocalization from the Cu^{II} ion towards the planar skeleton of the $\text{N}(\text{O})\text{--C--O}$ bridging part of the ligand. A similar situation occurs for the $\text{Cu}^{\text{II}}\text{--Ni}^{\text{II}}$ pair, with additional Ni^{II} local anisotropy treated with the phenomenological zero-field splitting. The resulting J is higher, and has been estimated at $J = -100 \text{ cm}^{-1}$. For other couples, for instance $\text{Cu}^{\text{II}}\text{--Co}^{\text{II}}$, $\text{Cu}^{\text{II}}\text{--Fe}^{\text{II}}$, and $\text{Cu}^{\text{II}}\text{--Ln}^{\text{III}}$, the orbital contribution renders the interpretation of magnetic data using the simple scheme described above extremely difficult. For these species only qualitative interpretation of magnetic data has been achieved in order to determine the nature of exchange interactions between Cu^{II} and the other ion.

Table 1. Bis-oxamato Cu^{II} building blocks and resulting bimetallic compounds (M stands for magnet and m for metamagnet).

Ligand skeleton (R)		R ₁ and R ₂	Ligand abbreviation	Cluster	Chain	Ladder	Plane	Interlocked planes	
$[\text{Cu}^{\text{II}}\text{L}]_2^{2-} = \left\{ \begin{array}{c} \text{---R---} \\ \diagup \quad \diagdown \\ \text{N} \quad \text{N} \\ \diagdown \quad \diagup \\ \text{O} \quad \text{O} \\ \diagup \quad \diagdown \\ \text{C} \quad \text{C} \\ \diagdown \quad \diagup \\ \text{O} \quad \text{O} \end{array} \right\}^{2-}$		Bimetallic compound							
	Y = OH Y = H	O O	pbaOH pba	✓	✓ (M) ✓ (m)				
	X = H	O	opba	✓	✓ (m)	✓ (M)	✓ (M)	✓ (M)	
	O and NMe NMe N-(CH ₂) _n -C ₆ H ₅ n = 1, 3, 4		Meopba Me ₂ opba PhMe ₂ opbox PhPr ₂ opbox PhBu ₂ opbox opbaCl ₂				✓ (M) ✓ (M) ✓ (M) ✓ (M) ✓ (M)		
	X = Cl	O	opbaCl ₂	✓					
		O	bis-pba	✓					

1.2.1.3 Discrete Molecules

One of the first high-spin molecules was prepared in 1988. By using $[\text{Cu}(\text{pba})]^{2-}$ as the core and $[\text{Mn}(\text{Me}_6\text{-[14]ane-N}_4)]^{2+}$ as a peripheral complex it is possible to obtain a trinuclear linear CuMn_2 species [5]. No single crystal was obtained, and a structure in agreement with the magnetic properties was proposed. The compound has ferrimagnetic behavior with an irregular spin state structure resulting from the antiferromagnetic interaction between the peripheral Mn ions ($S_{\text{Mn}} = 5/2$) and the middle Cu ion ($S_{\text{Cu}} = 1/2$). The low-temperature magnetic behavior is characteristic of a high-spin ground state equal to $S = 9/2$. Efforts were later made to obtain structural information for such species [9]. Let us mention the result of Liao's group. They succeeded in isolating crystals of binuclear and trinuclear compounds with the Ni^{II} ion ($S_{\text{Ni}} = 1$) [7]. The compounds are obtained by reaction of CuL^{2-} ($\text{L} = \text{pba}, \text{pbaOH}$ and opba) with NiL^{2+} , L being tetraamine ligands, the final compounds having formula $(\text{L Ni})\text{CuL}$ or $(\text{L Ni})_2\text{CuL}^{2+}$ (the trinuclear species is shown in Fig. 1). The compounds have been magnetically characterized, and have the expected ferrimagnetic behavior with an $S = 3/2$ ground state with a zero-field splitting.

An other interesting example has been described by Ouahab and Kahn with the opbaCl_2 ligand (Table 1) and its Cu^{II} complex [10]. The reaction of the Cu^{II} precursor with ethylenediamine, en, and Mn^{II} in the solvent DMSO led to an unprecedented trinuclear species $\text{Mn}^{\text{III}}\text{Cu}^{\text{II}}\text{Mn}^{\text{III}}$. The structure of this species has been resolved (Fig. 2), and reveals that:

- the Mn^{III} has replaced the Cu^{II} in the cavity N_2O_2 of the opbaCl_2 ligand;
- the formation of the $[\text{Cu}(\text{en})_2]^{2+}$ complex, because of the strong affinity of the en for the Cu^{II} ; and, finally,
- the self-assembling process between the anionic $[\text{Mn}(\text{opbaCl}_2)]^-$ and the cationic $[\text{Cu}(\text{en})_2]^{2+}$ complexes.

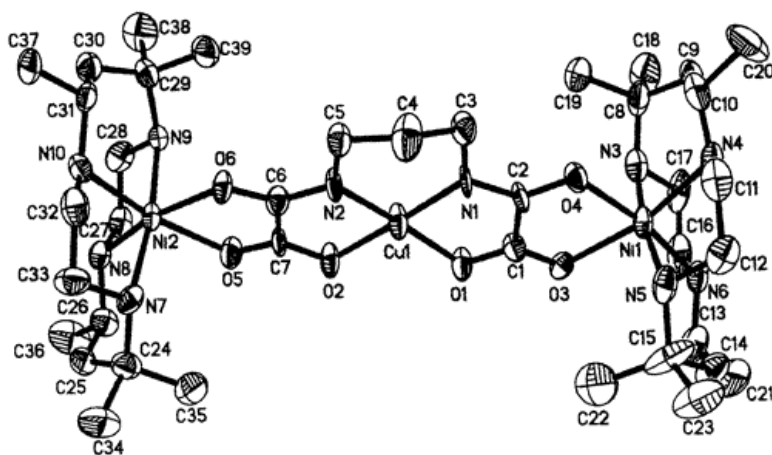


Fig. 1. Structure of the trinuclear cation $[\text{Ni}(\text{th})_2]\text{Cu}(\text{pba})^{2+}$ [7] (reproduced with permission; Copyright 2001, the American Chemistry Society).

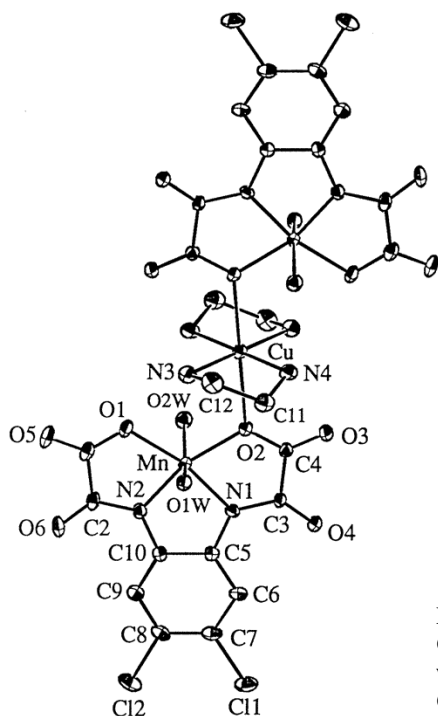
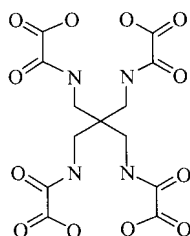


Fig. 2. Structure of the trinuclear species $\text{Cu}(\text{en})_2\text{Mn}(\text{Cl}_2\text{opba})(\text{H}_2\text{O})_2$ [10] (reproduced with permission; Copyright 2001, the American Chemistry Society).

The linkage between the two complexes is realized through apical Cu–O bonds of length 2.454 Å. The delocalization of the spin density of the Cu^{II} towards the oxygen atoms in the apical position has been postulated to be negligibly small, and the magnetic data have been interpreted in terms of zero-field splitting of the Mn^{III} ion.

More recently, Journaux et al. obtained an interesting dinuclear $\text{Na}_4[\text{Cu}_2(\text{bis-pba})]$ species by use of the bis-tetradentate ligand denoted bis-pba (Table 1 and Scheme 3) [11]. They succeeded in isolating dinuclear $\text{Na}_4[\text{Cu}_2(\text{bis-pba})]$ species, with weak intramolecular ferromagnetic interactions between the two Cu^{II} ($J \approx 1 \text{ cm}^{-1}$). The reaction of this dinuclear compound with four equivalent external complexes such as $[\text{Ni}(\text{cyclam})]^{2+}$ (cyclam = 1,4,8,11-tetraazacyclotetradecane) in acetonitrile or with $[\text{Cu}(\text{tmen})]^{2+}$ (tmen = *N,N,N,N*-tetramethylethylenediamine) in water affords hexanuclear anionic compounds of formula $\{\text{Ni}(\text{cyclam})\}_4\text{Cu}_2(\text{bis-pba})$ and $\{\text{Cu}(\text{tmen})(\text{H}_2\text{O})\}_2\{\text{Cu}_2(\text{bis-pba})\}$, respectively [12]. The structure of the Cu_6 species is shown in Fig. 3. It is made of two symmetry-related oxamato-bridged trinuclear units connected through the central carbon. In these hexanuclear species, the interactions through the oxamato bridge were found to be equal to $J = -342 \text{ cm}^{-1}$ for Cu_6 and -82 cm^{-1} for Cu_2Ni_4 . The weak ferromagnetic coupling between the two Cu^{II} ions within the dinuclear synthon was masked by intermolecular interactions and/or local anisotropy.

[Bis-pba]⁸⁻

Scheme 3

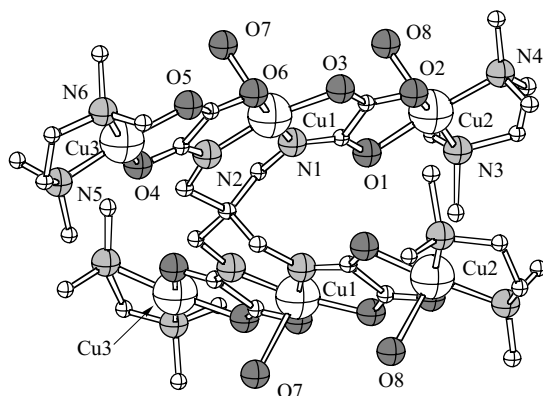


Fig. 3. Structure of the cationic hexanuclear unit $[\{\text{Cu}(\text{tmen})(\text{H}_2\text{O})\}_2\{\text{Cu}(\text{tmen})\}_2\{\text{Cu}_2(\text{bis-pba})\}]^{4+}$ [12] (reproduced with permission from Journal of Inorganic Chemistry).

1.2.1.4 One-dimensional Systems: Chain Compounds

When the dianionic Cu precursor is reacted with a 3d metal cation, M^{n+} , under stoichiometric conditions 1:1, neutral compounds of formula MCu_xS are obtained, S standing for solvent molecules. Different bimetallic chains have been structurally and magnetically described. The bimetallic chains with $M = \text{Mn}^{\text{II}}$ are described in detail in the review written in 1995 by Kahn. A typical example of a linear bimetallic chain is presented in Fig. 4. The magnetic properties of the chain compounds are well understood in the paramagnetic region (5–300 K), and are analyzed with theoretical models for ferrimagnetic one-dimensional systems, because of antiferromagnetic coupling between two different spins ($S_{\text{Mn}} = 5/2$ and $S_{\text{Cu}} = 1/2$) [13]. Below 5 K magnetic ordering occurs because of interchain interactions, which are governed by the crystal packing of the chains in the lattice. Actually, only one compound has ferromagnetic (F) ordering, with $T_{\text{C}} = 4.6$ K, namely $\text{MnCu}(\text{pbaOH})(\text{H}_2\text{O})_3$, which was the first molecule-based magnet belonging to the family described here [2]. Other compounds have antiferromagnetic (AF) ordering with T_{N} between 1.8 K and 5 K. The occurrence of F or AF magnetic ordering in these chain compounds is related to the interchain metal-metal separations of the type Mn–Cu for ferromag-

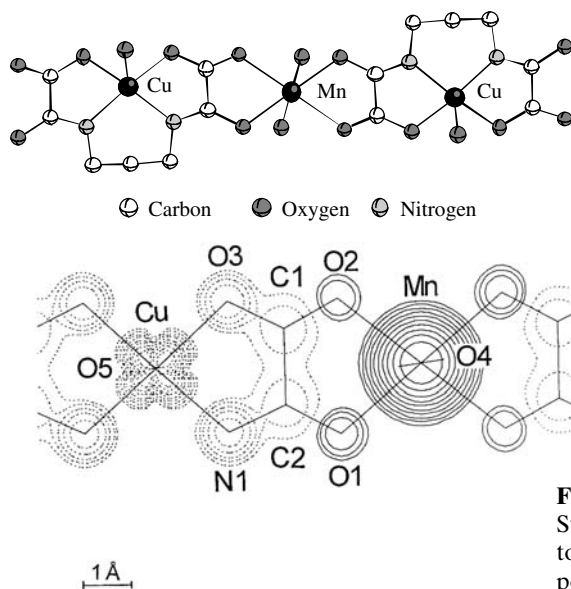


Fig. 4. MnCu(pba)(H₂O)₃ · 2H₂O (top) Structure of the chain compound (bottom) Spin density map deduced from polarized neutron diffraction data.

nets and Mn–Mn and Cu–Cu for antiferromagnets [14]. Some of these antiferromagnets behave as metamagnets, where a small applied magnetic field (between 1 or 2 kOe) can overcome the weak antiferromagnetic interchain interactions to induce a long-range ferromagnetic-like ordering. Note that for a few compounds there is no evidence of cooperative magnetic phenomena down to 1.8 K. They behave as quasi-perfect one-dimensional ferrimagnets; one example is MnCu(opba)(DMSO)₃ which has a zigzag chain structure [15].

Two interesting features of these bimetallic chain compounds can be mentioned in this section. First, the size of crystals (up to 15 mm³) of [MnCu(pba)(H₂O)₃] · 2H₂O (Fig. 4) enabled the performance of further physical studies such as polarized neutron diffraction (p. n. d.) and optical spectroscopy (Section 1.2.4) [16, 17]. Secondly, the magnetic properties of compounds of formula [MnCu(pbaOH)] · xH₂O are strongly dependent on the water composition. Just above we mentioned the compound MnCu(pbaOH)(H₂O)₃, which behaves as a magnet at 4.6 K. It is possible to isolate another phase of this compound, MnCu(pbaOH)(H₂O)₃ · 2H₂O, which has three-dimensional antiferromagnetic ordering in zero fields with $T_N = 2.4$ K. The bimetallic chains in both compounds are identical but in the latter the hydrogen-bond network developed by the non-coordinated water molecules imposes crystal packing with short interchain Mn–Mn and Cu–Cu separations, inducing antiferromagnetic interactions between the chains. The compound also has metamagnetic behavior, because a field of 0.9 kOe is sufficient to overcome these interchain interactions giving rise to a ferromagnetic state [14]. When MnCu(pbaOH)(H₂O)₃ is heated to 130°C one water molecule bound in the apical position of the copper coordination sphere is removed, and the new compound, MnCu(pbaOH)(H₂O)₂, has long range ferromagnetic ordering at $T_C = 30$ K [18]. The release of H₂O reduces

the interchain distances, and this enhances the interchain exchange interactions by a factor of 40. In Section 1.2.3 we will encounter other examples of magnetic ordering controlled by the water content of the material; these lead to the concept of magnetic sponges.

1.2.1.5 Two-dimensional Systems: Layered Honeycomb Compounds

We have seen that magnetic ordering of chain compounds can occur, and is strongly related to solvent molecules which impose the organization of the crystal packing. The interchain magnetic interactions remain weak, however, and magnetic ordering occurs at low temperature. To increase these temperatures, chemists have to build compounds with higher dimensionality. This section is devoted to bidimensional compounds, which are prepared with the same building blocks as the one-dimensional compounds but with different stoichiometries. Almost all of these 2D compounds behave as ferrimagnets. Experimentally the long-range magnetic ordering is revealed by the temperature dependencies of the field-cooled magnetization (FCM, which is measured by cooling the sample within a very small field, usually $H < 20$ Oe) and by the in-phase (χ'_M) and out-of-phase (χ''_M) molar susceptibilities in the ac mode. The non-zero value of χ''_M indicates the presence of permanent magnetic moment within the sample. The critical temperatures, denoted T_C , are determined by the extremum of the derivative curve $d(\text{FCM})/dT$ or by the maximum of the χ'_M curve, if it exists. In both instances they correspond to the temperatures where remnant magnetization vanishes, the latter is measured by turning the field off at low temperature and then warming up the sample in strictly zero field. The field dependence of the magnetization measured at low temperature enables the determination of the coercive field.

The reaction of $(\text{NBu}_4)_2[\text{Cu}(\text{opba})]$ with Mn^{II} in DMSO in 3:2 stoichiometry yielded a compound of formula $(\text{NBu}_4)_2[\text{Mn}_2\{\text{Cu}(\text{opba})\}_3,4\text{DMSO}] \cdot 2\text{H}_2\text{O}$, which is a ferrimagnet below $T_C = 15$ K [15]. When Mn^{II} is replaced by Co^{II} , T_C increases to 29 K [19]. Unfortunately, no crystals were obtained for these compounds; a layered honeycomb structure was proposed for the anionic part (Fig. 5), for compatibility with the chemical formulas of the compounds and, of course, with the magnetic ordering occurring for temperatures higher than for the chain compounds. A theoretical approach was developed for a two-dimensional hexagonal model to derive an analytical expression for the molar magnetic susceptibility, χ_M , in the paramagnetic regime (40–300 K) using high-temperature expansions of the partition function [20]. Comparison of theory and experiment led to determination of the exchange parameter as $J = -33.1 \text{ cm}^{-1}$, which is close to values obtained for related finite or chain compounds.

The occurrence of magnetic ordering in these two dimensional compounds might result from intralayer magnetic anisotropy and/or interlayer interactions. The cations are probably located between the anionic layers, and it is possible that the magnetic properties of these materials can be tuned by changing the size of the cations and/or slight modification of the ligand. Table 2 summarizes the different results. The magnetic behavior of the Mn derivatives strongly depends on the size

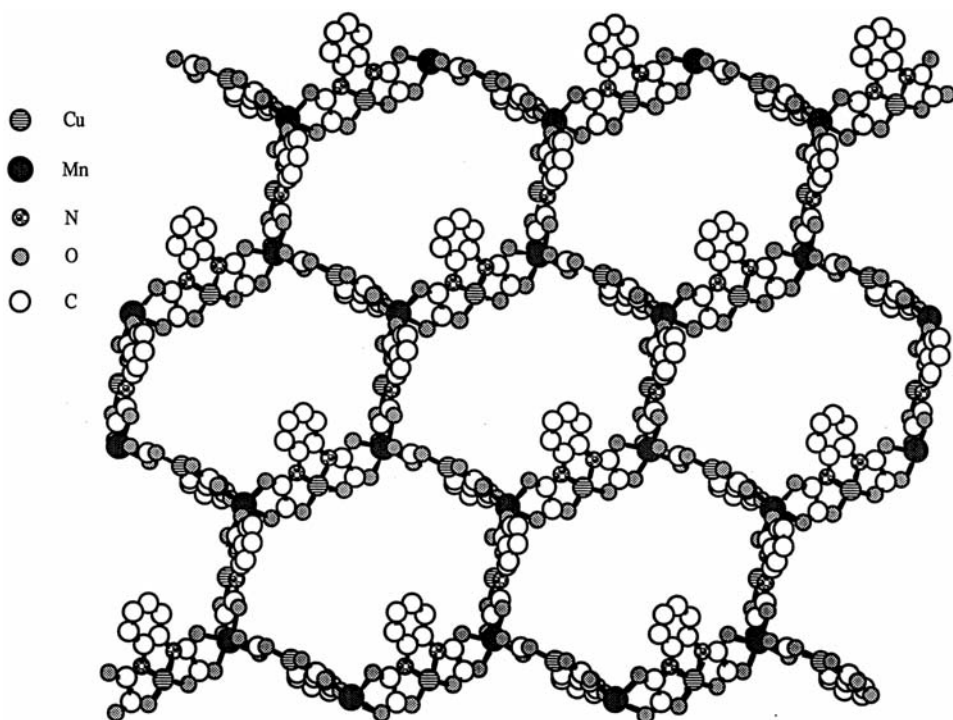


Fig. 5. Structure of a honeycomb layer.

of the cations. For large cations such as $[\text{Ru}(\text{bipy})_3]^{2+}$ magnetic ordering occurs at lower temperature [21], and for small cations such as alkali metals, the compounds have weak ferromagnetism [19], because of competition between antiferromagnetic interlayer interactions and ferrimagnetic intralayer interactions. In contrast, all the Co compounds are ferrimagnets with $T_C \approx 30$ K, irrespective of the cation. Such similar magnetic properties strongly suggests that the compounds adopt the same structure.

For some of these compounds XANES and EXAFS studies showed that each Mn^{II} is surrounded by three CuL complexes [22]. Journaux et al. compared experimental magnetic data with two theoretical models. One is based on a two-sublattice molecular field model in the mean field approximation, and is assumed valid for three-dimensional structures. The second already introduced above is adapted for hexagonal honeycomb layers. For all the examples studied the second approach led to good fitting of the magnetic data, and gave J values in good agreement with those deduced previously for other compounds of lower dimensionality. These structural and magnetic results lead to the conclusion that all these compounds are two-dimensional, with a honeycomb layered structure.

Finally, introduction of a cation with an intrinsic property, for instance chirality for cations such as nicot andambutol or the paramagnetic $[\text{FeCp}_2^*]^+$, has been envisaged [23, 24]. Chirality was introduced with the objective of inducing the for-

Table 2. Magnetic properties for the family of oxamato(oxamido)-bridged honeycomb layered ferrimagnets of formula $\text{Cat}_2^{\text{I}}[\text{M}_2^{\text{II}}(\text{CuL})_3]$ and $\text{Cat}^{\text{II}}[\text{M}_2^{\text{II}}(\text{CuL})_3]$.

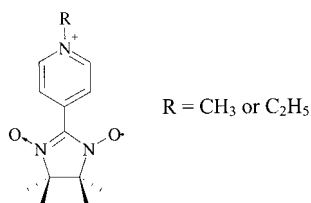
M^{II}	L	Cat	J (cm^{-1})	T_{C} (K)	H_{coerc} (Oe)	Ref.		
Mn	opba	NBu_4^+	-32	15	<10	[15]		
		NEt_4^+		17	<10	[19]		
		NMe_4^+			$T_{\text{N}} = 15$ K	[19]		
		K^+			$T_{\text{N}} = 15$ K	[19]		
		Na^+			$T_{\text{N}} = 15$ K	[19]		
		FeCp_2^{*+}		14		<20	[24]	
		CoCp_2^{*+}		13		<20	[24]	
		<i>nicot</i> $^{2+}$			$T_{\text{N}} = 15$ K		[23]	
		<i>ambutol</i> $^+$			$T_{\text{N}} = 15$ K		[23]	
		$\text{Ru}(\text{bipy})_3^{2+}$			12		[21]	
				PPh_4^+	-31.8	11.5	10	[22]
			Meopba	PPh_4^+	-32.6	13	10	[22]
			Me_2opba	PPh_4^+	-30.5	8	10	[22]
			$\text{PhMe}_2\text{opbox}$	PPh_4^+		12.5	5	[26]
	$\text{PhPr}_2\text{opbox}$	PPh_4^+		11.5	5	[26]		
	$\text{PhBu}_2\text{opbox}$	PPh_4^+		13.5	5	[26]		
Co	opba	NBu_4^+		30.5	1400 (5 K)	[15]		
		NMe_4^+		33		[19]		
		Cs^+		34		[19]		
		K^+		33.5	2000 (5 K)	[19]		
		Na^+		31.5		[19]		
		FeCp_2^{*+}		27	3500	[24]		
		CoCp_2^{*+}		27.5	5300	[24]		

Notes: $\text{Cp}^* = \text{C}_5\text{Me}_5$, *nicot* is the chiral *N,N*-dimethylnicotinium species and *ambutol* is the chiral dimethylhydroxymethyl-2-ethylhydroxymethyl-1-propylammonium species.

mation of three dimensional coordination polymers in the same manner as for the 3D lattices obtained for the oxalato-bridged family discussed in another chapter of this series [25]. The magnetic cation was expected to increase the magnetic interaction between the layers, but the results were slightly disappointing, because no significant modifications of the magnetic properties were observed. These observations are, however, informative because they suggest future directions which might afford three-dimensional molecule-based magnets. In fact, a chiral cation can induce the formation of magnetic helicates only if it correctly fills the cavities formed by the three dimensional lattice. This obviously did not happen with the examples given above. Another way of filling the cavities of the anionic network is to use bulky ligands. The results obtained with the bulkier PhR_2opbox ligands (Table 1) designed on the basis of this strategy are not conclusive [26]. Note that the compound obtained with $[\text{FeCp}_2^*]^+$ enabled a Mössbauer study which revealed that the Fe^{III} ion begins to feel an internal field only at temperatures well below T_{C} . This clearly indicates that the cation between the layers is not directly involved in the long range magnetic ordering.

1.2.1.6 Interpenetrated Two-dimensional Networks: Interlocked Compounds

To increase the dimensionality further Kahn and coworkers imagined the use of a cation which would be capable of bridging two transition metal ions and which would be paramagnetic, thus increasing the magnetic density of the compounds. Cations belonging to the nitronyl nitroxide family, in which the unpaired electron is equally shared between the two N-O groups, have been envisaged (Scheme 4).



Scheme 4

The methyl and ethylpyridinium radical cations were used with success [27-29]. The structures of compounds with the formula (Etrad)₂[M₂{Cu(opba)}₃] have been investigated by single crystal X-ray studies for M = Mn, Co, and by powder X-ray studies for M = Mg, Ni [30, 31]. All the compounds are fully interlocked with a general architecture made of two equivalent two-dimensional networks, denoted A and B, each consisting of parallel honeycomb layers. Each layer is made up of edge-sharing hexagons with an M^{II} ion at each corner and a Cu^{II} ion at the middle of each edge (Fig. 5). The layers stack above each other in a graphite-like fashion, with a mean interlayer separation of 14.8 Å. The A and B networks are almost perpendicular to each other, and interpenetrate in such a way that at the center of each hexagon belonging to a network is located a Cu^{II} ion belonging to the other network (Fig. 6). The networks are further connected through the radical cations; this affords infinite chains of the kind Cu_A-Etrad-Cu_B-Etrad, where Cu_A and Cu_B belong to the A and B network, respectively.

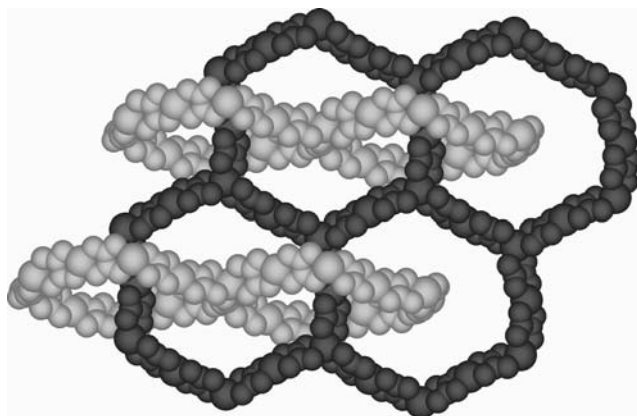


Fig. 6. Interpenetration of the two networks A and B.

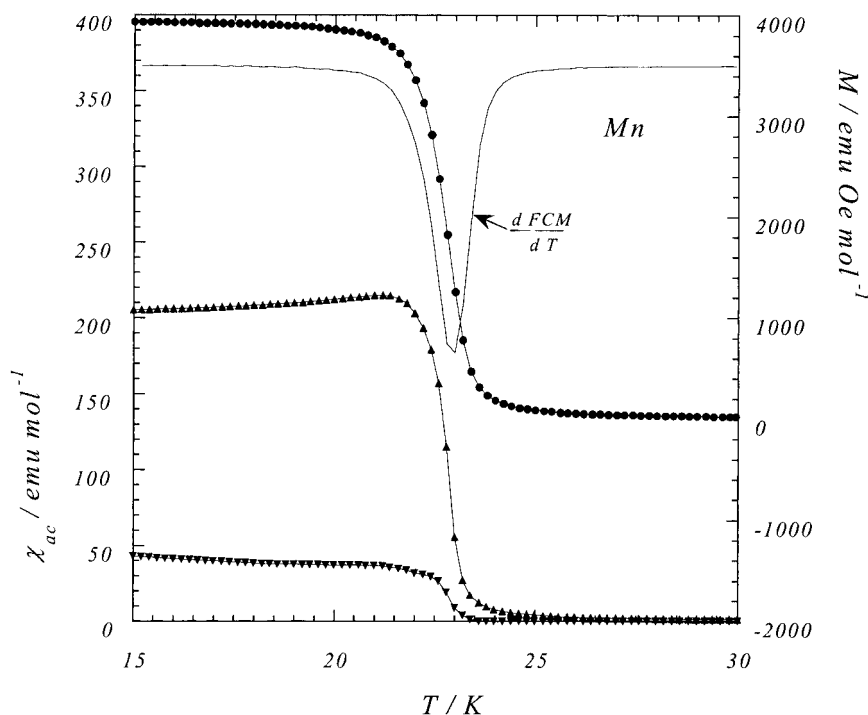


Fig. 7. FCM curve (●) and its derivative $d(\text{FCM})/dT$ (top) and in-phase χ'_M (▲) and out-of-phase χ''_M (▼) plots of ac susceptibilities (bottom) against T for $(\text{Etrad})_2[\text{Mn}_2\{\text{Cu}(\text{opba})\}_3]$.

Besides the aesthetic aspect of the structures, the compounds also had interesting magnetic properties. They behave as ferrimagnets with Curie temperatures in the range of 22–37 K (Figs. 7 and 8 and Table 3). The χ'_M and χ''_M curves can have two different general shapes, (i) a shape similar that of the FCM with $\chi'_M \gg \chi''_M$ as shown in Fig. 7, or (ii) a peak-like shape as shown in Fig. 8 with maximum values for very close temperatures. These differences are related to the coercivity of the material, case (i) applies for a very weak coercivity ($H_{\text{coerc}} < 10$ Oe) and case (ii) when a

Table 3. Magnetic properties for the family of oxamato(oxamido)-bridged interlocked ferrimagnets of formula $(\text{r-Rad})_2[\text{M}_2^{\text{II}}(\text{CuL})_3]$, where r = methyl- or ethylpyridinium.

M^{II}	L	Cat	T_C (K)	H_{coerc} (Oe)	Ref.
Mn	opba	Merad	23	<10	[15]
		Etrad	22.8	<10	[29]
Co	opba	Merad	34	3000 (5 K)	[15]
		Etrad	37	8500–24 000	[29]
Ni	opba	Etrad	28	500	[30, 31]
Mg	opba	Etrad	Paramagnet	Paramagnet	[31]

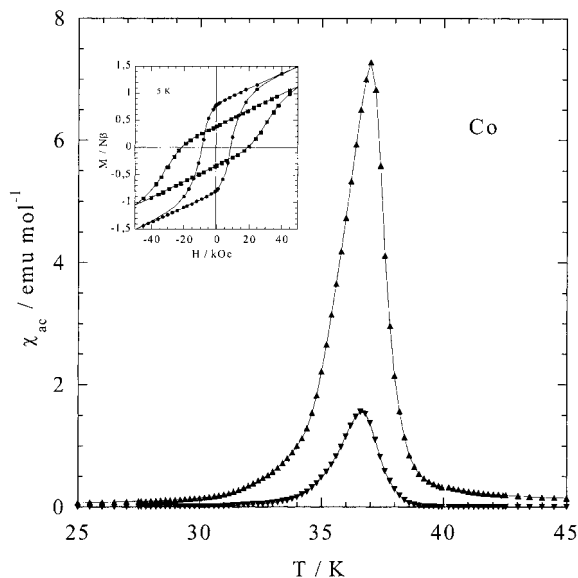


Fig. 8. In-phase χ'_M (\blacktriangle) and out-of-phase χ''_M (\blacktriangledown) ac susceptibilities (bottom) for $(\text{Etrad})_2[\text{Co}_2\{\text{Cu}(\text{opba})\}_3]$. The insert shows the field dependence of the magnetization for two samples with the largest (\bullet) crystals and smallest (\blacksquare) crystals.

significant coercivity ($H_{\text{coerc}} > 1000$ Oe) exists. As a result of the formation of the 3D networks the Curie temperatures are effectively increased by up to 8 K for the Mn and Co compounds, compared with the layered compounds (Table 2). But the increase of T_C seems weak with regard to the three-dimensional connectivity of the compound. In fact, the interaction between the interlocked layers is weak, and has been estimated in $(\text{Etrad})_2[\text{Mg}_2\{\text{Cu}(\text{opba})\}_3]$. Because the Mg ion is diamagnetic, magnetic interactions occur only along the $\text{Cu}_A\text{-Etrad-Cu}_B\text{-Etrad}$ chains. They are ferromagnetic, as expected between Cu^{II} and a nitroxide group occupying the apical position. Neglecting intermolecular interactions, the magnetic data were analyzed by a chain model for $S = 1/2$ spins, leading to an exchange parameter of $J = 8 \text{ cm}^{-1}$, which is four times weaker in absolute values than the intralayer interaction [31].

1.2.1.7 Ladder and Honeycomb Lattices in 3d-4f Systems

The chemistry of the bis-bidentate Cu-oxamato complexes is not limited to the reaction with 3d transition metals. Impressive extended structures have been obtained when $[\text{Cu}(\text{opba})]^{2-}$ was reacted with lanthanide ions, Ln^{III} . The first compounds of this kind were reported in 1992 for the $\text{Ln}^{\text{III}}\text{-Cu}(\text{pba})$ system [32]. Two different structures have been described for compounds of general formula $\text{Ln}_2\{\text{Cu}(\text{pba})\}_3$. One consists of discrete ladders of Ln going from Tb to Yb, and Y, an architecture similar to that of $\text{Ln}_2\{\text{Cu}(\text{opba})\}_3$ shown in Fig. 9. The second results from condensed ladder-like motifs with a rearrangement of the rungs and is formed with Ln